Segregation-pattern reorientation of a granular mixture on a horizontally oscillating tray

Masashi Fujii,* Akinori Awazu, and Hiraku Nishimori
Department of Mathematical and Life Sciences, Hiroshima University, Kagamiyama, Higashi-Hiroshima 739-8526, Japan
(Received 12 December 2011; published 16 April 2012)

Reorientation of the segregation pattern of a binary granular mixture on a two-dimensional horizontally oscillating tray is numerically realized. The mixture consists of large and heavy particles and small and light particles, and the segregation pattern shows a transition between a striped pattern perpendicular to the oscillation and one parallel to the oscillating direction according to the change of area fractions of the two types of particle. The transition mechanism is discussed on the basis of a simplified one-dimensional dynamics.

DOI: 10.1103/PhysRevE.85.041304 PACS number(s): 45.70.Mg, 82.35.Jk

Granular materials exhibit various complex behaviors, and their characteristic dynamics has been studied extensively in, for instance, the crystallization of granular materials [1] or the pattern formation of granular mixtures on a horizontally oscillating tray [2–5], in a horizontally rotating drum [6–11], and in a vertically oscillating box [12,13]. However, thus far, research on the basic physics of granular dynamics as well as macroscopic phenomenology has been insufficient. For example, previous studies on the pattern formation of a granular mixture on a horizontally oscillating tray [2–5] have demonstrated that different types of granular material segregate to form a stripe pattern that extends perpendicularly to the oscillating direction, while no segregated pattern has been observed parallel to the oscillating direction. The potential possibility of the emergence of the latter segregation pattern has been an intriguing issue in this field of study. For a wider range of soft materials, a recent numerical study on a colloidal mixture found stripe patterns that were both parallel and perpendicular to the oscillating electric field [14]. In this study, we use a numerical model and show that transition between steady perpendicular and steady parallel stripe patterns can be observed in a granular mixture as well, for a suitable set of parameters and a suitable combination of the area fractions of the two types of constituting particle.

We employ the distinct element method [3,4] and simulate the behaviors of the granular mixture on a two-dimensional horizontally oscillating tray. This mixture consists of two types of particle: (i) particles with a large grain size and mass, which we refer to as L particles, and (ii) particles with a small grain size and mass, which we refer to as S particles (see Table I). The ith particle has type-dependent mass (m_i^{type}) and size (D_i^{type}) ($type = L$ or S), and its position is denoted by a two-dimensional vector $\mathbf{r}_i$ [$=(x_i, y_i)$]. Each particle is subjected to viscous friction, which is proportional to the velocity difference between the particle and the tray with the friction coefficient μ [3,4]. If the ith and jth particles overlap, the interaction is indicated by a linear elastic force with viscous dissipation, depending on the combination of the types of particle; the elastic coefficient and the coefficient of dissipation are denoted as k and $\gamma_{i,j}$, respectively. Here, $\gamma_{i,j}$ is derived from the coefficient of restitution $e^{i,j}$, the elastic coefficient k, and the reduced mass of the particles as follows:

$$\gamma_{i,j} = -\frac{2\ln e_{i,j}\sqrt{k\frac{m_i m_j}{m_i+m_j}}}{\sqrt{\pi^2+(\ln e_{i,j})^2}}. \tag{1}$$

The dynamic equation of the ith particle is summarized as

$$m_i^{\text{type}}\ddot{\mathbf{r}}_i = \sum_{j\neq i}\mathbf{f}_{i,j} - \mu(\dot{\mathbf{r}}_i - \dot{\mathbf{r}}_{\text{tray}}), \tag{2}$$

$$\mathbf{f}_{i,j} = \begin{cases} k\frac{\delta\mathbf{r}_{i,j}}{|\delta\mathbf{r}_{i,j}|}\left[\frac{D_i^{\text{type}}+D_j^{\text{type}}}{2} - |\delta\mathbf{r}_{i,j}|\right] - \gamma_{i,j}\dot{\delta\mathbf{r}}_{i,j} \\ \quad \text{for} \quad |\delta\mathbf{r}| \leqslant \left(D_i^{\text{type}}+D_j^{\text{type}}\right)/2 \\ 0 \quad \text{for} \quad |\delta\mathbf{r}| > \left(D_i^{\text{type}}+D_j^{\text{type}}\right)/2, \end{cases} \tag{3}$$

$$\delta\mathbf{r}_{i,j} = \mathbf{r}_i - \mathbf{r}_j, \tag{4}$$

where the velocity of the tray is given as

$$\dot{\mathbf{r}}_{\text{tray}} = (\dot{x}_{\text{tray}}, \dot{y}_{\text{tray}}) = (2\pi A\nu\sin(2\pi\nu t), 0). \tag{5}$$

Note that the rotation of the particle is not considered. The values of the parameters are summarized in Table I; most of them are set the same as or close to those introduced in previous related studies [3,4]. As one exception, the elastic coefficient k is set smaller than in previous studies, meaning that the particles are not so rigid, but the collision time derived from the elastic coefficient remains small compared with the period of oscillation of the tray. In addition, for simplicity, we consider only the case where the elastic coefficients of the L and S particles are identical. Another exception is the large value of μ, assuming that the particles are more strongly affected by the viscous friction arising from their velocity relative to the tray than in previous studies. This is done to explore potentially new aspects of the segregation dynamics on a horizontally oscillating tray. Random fluctuations in the system are neglected. Systematic calculations to verify the effect of viscous friction on segregation will be presented later.

We perform simulations using several combinations of N_L and N_S, i.e., the number of L and S particles, respectively. In addition, we define the area fractions of L and S particles as $\rho_L \equiv N_L\pi(D^L)^2/(4W^2)$ and $\rho_S \equiv N_S\pi(D^S)^2/(4W^2)$, respectively. The width of the system is $W = 40$ cm in both the oscillational and lateral directions, and periodic boundary conditions are set in both directions. Each run starts from $t = 0$, when the particles are randomly distributed on a tray without overlap, and ends at $t = 200$.

*mfujii0123@hiroshima-u.ac.jp

TABLE I. Parameter values considered in numerical simulation for pattern transformation.

Property	L value	S value
m^{type} (mass)	$m^L = 1$ g	$m^S = 0.025$ g
D^{type} (size)	$D^L = 1$ cm	$D^S = 0.5$ cm
Property		**Value**
$e^{\text{type}_i,\text{type}_j}$ (type of i, type of j)		
(L,L)		$e^{L,L} = 0.2$
(L,S) or (S,L)		$e^{L,S} = 0.5$
(S,S)		$e^{S,S} = 0.9$
μ (friction coefficient)		1 g s^{-1}
k (elastic coefficient)		1.0×10^4 g cm^2 s^{-2}
A (amplitude of oscillation of tray)		10 cm
ν (frequency of oscillation of tray)		2 Hz

Figure 1 shows typical patterns emerging as steady states of the binary granular particle mixtures: (a) nonstripe pattern, (b) stripe pattern perpendicular to the oscillating direction (hereafter, we refer to this pattern as the perpendicular-striped pattern), (c) stripe pattern parallel to the oscillating direction (hereafter, we refer to this pattern as the parallel-striped pattern), and (d) crossed-striped pattern.

To distinguish these four patterns quantitively, we define a temporal order parameter $\Phi(t)$. Specifically, the system is separated into $M \times M$ ($M = 40$) square cells and a quantity

$$\sigma_{i,j}(t) = N^L_{i,j}(t)(D^L)^2 - N^S_{i,j}(t)(D^S)^2, \tag{6}$$

is allocated to each cell (i,j), where $N^L_{i,j}(t)$ and $N^S_{i,j}(t)$ are, respectively, the numbers of L and S particles in cell (i,j) at

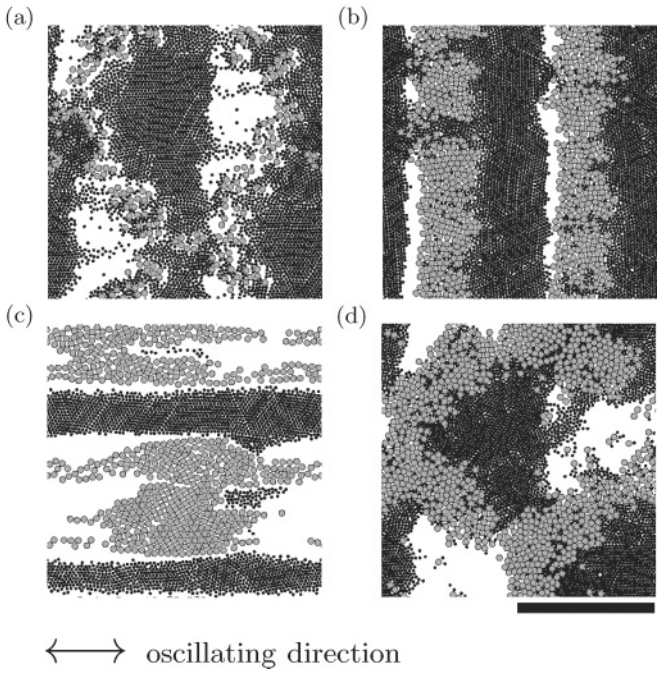

FIG. 1. Typical steady states of particle mixtures: (a) nonstripe pattern ($\rho_L = 0.1, \rho_S = 0.65$); (b) stripe pattern perpendicular to oscillating direction ($\rho_L = 0.30, \rho_S = 0.55$); (c) stripe pattern parallel to oscillating direction ($\rho_L = 0.30, \rho_S = 0.25$); and (d) crossed-striped pattern ($\rho_L = 0.40, \rho_S = 0.40$). The scale bar denotes 20 cm.

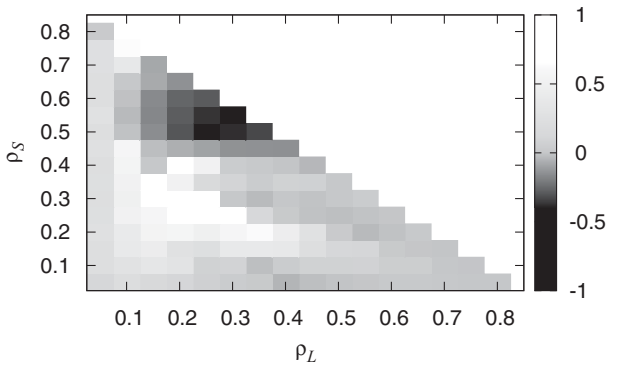

FIG. 2. Relationship between the order parameter Φ_{av} and the area fractions of L particles (horizontal axis) and S particles (vertical axis), for $A = 10$ and $\nu = 2$. A light color implies that Φ_{av} is close to 1, indicating the emergence of a parallel-striped pattern, and a dark color implies that Φ_{av} is close to -1, indicating the emergence of a perpendicular-striped pattern.

t. Then the specific form of the temporal order parameter $\Phi(t)$ is given as

$$\Phi(t) = \sum_j \sum_k \frac{\sum_i [\sigma_{i,j}(t)\sigma_{i+k,j}(t)]}{M^2 \sum_i [\sigma_{i,j}(t)^2]} - \sum_i \sum_k \frac{\sum_j [\sigma_{i,j}(t)\sigma_{i,j+k}(t)]}{M^2 \sum_j [\sigma_{i,j}(t)^2]}. \tag{7}$$

The first and second terms of the right-hand side of Eq. (7) quantify the spatial correlations along the directions parallel and perpendicular to the oscillating direction, respectively. In simple terms, $\Phi(t)$ approaches 1 when the parallel-striped pattern is dominant, whereas it approaches -1 when the perpendicular-striped pattern is dominant.

Simulations are systematically performed by varying the combination of $\rho_L \in \{0.05, 0.1, 0.15, \ldots, 0.8\}$ and $\rho_S \in \{0.05, 0.1, 0.15, \ldots, 0.8\}$, maintaining $\rho_S + \rho_L \leqslant 0.85$. The relationship between (ρ_L, ρ_S) and Φ_{av}, with $\Phi(t)$ averaged over the last 20 periods of oscillation, for $A = 10$ and $\nu = 2$ is shown in Fig. 2. As shown in the figure, to observe this relationship, we consider four typical regions: (a) $\rho_L \leqslant 0.1$ or $\rho_S \leqslant 0.1$, where Φ_{av} is close to zero; (b) $\rho_L + \rho_S \leqslant 0.85$, $\rho_L \geqslant 0.15$, and $\rho_S \geqslant 0.45$, where Φ_{av} is close to -1; (c) $\rho_L + \rho_S \leqslant 0.55$, $0.15 \leqslant \rho_L \leqslant 0.40$, and $0.15 \leqslant \rho_S \leqslant 0.35$, where Φ_{av} is close to 1; and (d) $0.55 \leqslant \rho_L + \rho_S \leqslant 0.85$ and $0.20 \leqslant \rho_S \leqslant 0.40$, where Φ_{ave} is close to zero. In region (a), particles tend not to form any stripe pattern, and in regions (b), (c), and (d), particles tend to form the perpendicular-striped, the parallel-striped, and the crossed-striped patterns, respectively.

It should be noted that the parallel-striped pattern obtained in region (c) has not been realized to our knowledge in previous studies on horizontally oscillating granular mixtures, wherein much lower viscous friction ($\mu \sim 0.1$) was used. To verify the effect of high viscous friction, $\mu = 1$, considered in the above calculations, as shown in Fig. 3, we calculate the order parameter in steady state with a varying combination of friction coefficients of L and S particles, keeping $\rho_L = 0.25$, $\rho_S = 0.3$, $A = 10$, and $\nu = 2$. The case of $\mu_L = \mu_S = 1$ in this figure corresponds to the case of $\rho_L = 0.25, \rho_S = 0.3$

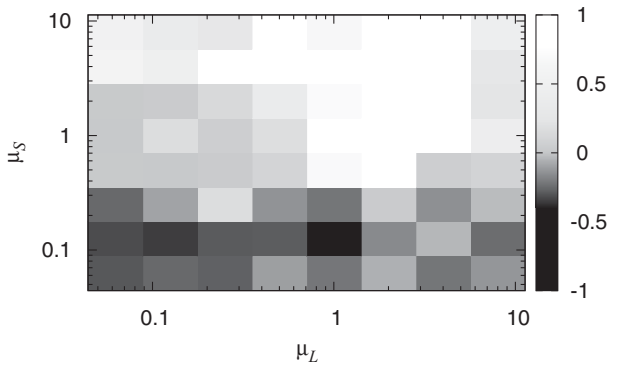

FIG. 3. Relationship between the order parameter Φ_{av} and the friction coefficients of L particles (horizontal axis, logarithmic scale) and S particles (vertical axis, logarithmic scale), for $\rho_L = 0.25$, $\rho_S = 0.3$, $A = 10$, and $\nu = 2$. A light color implies that Φ_{av} is close to 1, indicating the emergence of a parallel-striped pattern, and a dark color implies that Φ_{av} is close to -1, indicating the emergence of a perpendicular-striped pattern.

in Fig. 2. As roughly shown in Fig. 3, particles tend to form the parallel-striped pattern in the high-viscous-friction range and the perpendicular-striped pattern in the low-viscous-friction range. This is the reason why we choose the set $\mu_L = \mu_S = 1$ of viscous friction coefficients in this study; with this set we can see the present characteristic segregation dynamics approaching the parallel-striped pattern. Now, we focus on the time evolution of $\Phi(t)$ in region (c) of Fig. 1. Figures 4(b)–4(e) show simulation snapshots at $t = 0$, 30, 60, and 70, respectively, at $(\rho_L, \rho_S) = (0.3, 0.25)$; there, the gray particles correspond to L particles and the black particles to S particles. In the early stages of the simulation, $0 < t \leqslant 30$, the particles temporarily form a perpendicular-striped-like pattern as shown in Fig. 4(c), where the value of $\Phi(t)$ is kept around zero. In this stage, the perpendicular-striped pattern arises, but the alignments of stripes are not so distinct. In the next stage, $t = 30$ until $t = 90$, the value of $\Phi(t)$ gradually increases, and accordingly the striped pattern is greatly deformed to form clusters of L particles. For example, after $t = 60$, perpendicular stripes are hardly recognizable, as seen in Fig. 4(d); instead, a wedge of a horizontally extending cluster of S particles is seen to penetrate into the the clusters of L particles and serves as the seed for the parallel-striped pattern. Subsequently, another horizontal wedge of S particles begins to collide with the clusters of L particles to form second parallel stripe as seen in Fig. 4(e) for $t = 70$. Around $t = 90$, $\Phi(t)$ reaches a saturation value of $\Phi(t) \simeq 0.55$. Before this time the parallel-striped pattern has been established. Once the system reach this state the perpendicular movement of the particles is restricted by the strong friction force acting between the particles and the horizontally oscillating tray. Hence, the movements of L and S particles become synchronized, resulting in a sharp decrease in the frequency of particle collisions. In this way, the deformation of perpendicular stripes, which are formed at one time in the system, irrespective of the final pattern, plays a key role in the selection of the final pattern. In particular, considering the far more active movement of S particles than of L particles, which causes the deformation of the perpendicular

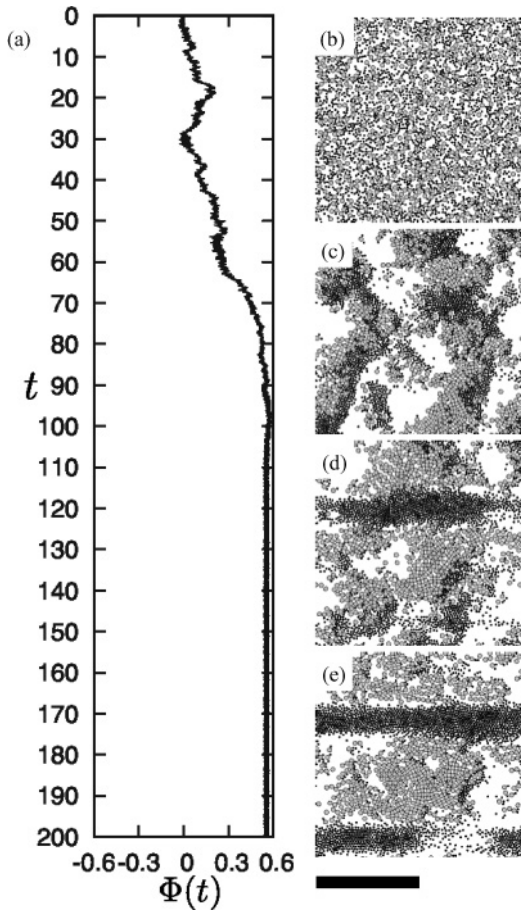

FIG. 4. (a) Time evolution of the order parameter, $\Phi(t)$, for $\rho_L = 0.30$ and $\rho_S = 0.25$, and the corresponding simulation snapshots at (b) $t = 0$, (c) 30, (d) 60 and (e) 70. The scale bar denotes 20 cm for (b)–(d).

alignment of the L particles, the stability of stripes of L particles against collisions with the cluster of S particles seems essential for the selection of the final pattern: perpendicular or parallel striped.

Accordingly, to investigate the stability of L-particle stripes (clusters) in a simplified setup, we consider a one-dimensional (1D) granular system, in which particles arrayed in the x (oscillating) direction share a central axis, as shown in Fig. 5; the L and S particles are kept unmixed. This is the 1D expression of the pattern of a pair of perpendicular stripes realized in the 2D system. The dynamics and external force are kept the same as in the 2D system, where the boundary condition is periodic. Note that because of the dimensionality, the sequence of particles is preserved in the 1D simulation. In this situation, we do not focus on the stability of the initial sequence of the L and S particles but on the stability of the

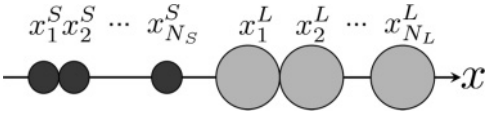

FIG. 5. Illustration of the system with a one-dimensional model. The small black circles represent the S particles and the large gray circles the L particles.

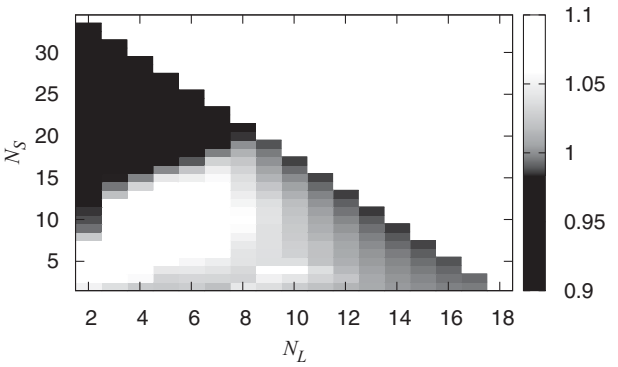

FIG. 6. Relationships among N_L (horizontal axis), N_S (vertical axis), and x_{av}^L. A very dark color indicates that the value of x_{av} is smaller than 1. A lighter color indicates that the value of x_{av}^L is larger than 1.

agglutinated state of the L particles. This agglutinated state of the L particles corresponds to a rigid structure of individual perpendicular stripes.

To quantify the agglutination degree of the L particles in the steady state of the system, we measure the mean distance between neighboring L particles,

$$x_{av}^L = \frac{1}{\tau}\int_{\tau}^{T} \frac{\left[x_{N_L}^L(t) - x_1^L(t)\right] \mathrm{mod}\ (W)}{N_L - 1} dt, \qquad (8)$$

where W (=20) is the total length of the system.

The relationship among N_L, N_S, and x_{av}^L obtained by the simulation is shown in Fig. 6. The very dark color indicates that the value of x_{av} is smaller than 1, the lighter color that the value of x_{av}^L is larger than 1. In this figure, we see three typical regions. In the cases where $N_S < 15$ and $N_L < 9$, the mean distance between the L particles is larger than 1; in other words, the L particles cannot be kept agglutinated in this region. It should be noted that, in this region, L and S particles frequently collide at the boundaries. In contrast, in the case where $N_S \geqslant 20$, the obtained values of x_{av}^L are smaller than 1, implying that the agglutinated state of L particles is stably maintained. In this case, the frequency of the collisions between the S and L particles is much lower than that in the previous case. In the case where $N_L > 10$, x_{av}^L takes intermediate values close to 1. These results suggest that the destabilization of the agglutinated state of L particles in the 1D simulation is realized for small spatial densities of L and S particles; this destabilization of the agglutinated state roughly corresponds to the unstable condition of perpendicular stripes of L particles in 2D simulation shown in Fig. 2. On the other hand, in the high-density regions of the 1D and 2D simulations, particularly in the high-density regime of S particles, the agglutinated state of the L particles is stable. Thus, the formation of the parallel-striped pattern is caused by the destabilization of the L-particle stripes. This destabilization requires frequent collisions of S particles with, that is, momentum transfer of S particles to, the L-particle striped structure. This momentum transfer is realized when S particles move actively in the region, allowing a proper combination of the area fractions of S and L particles. The two destabilization processes are to be investigated in greater detail in future research.

We numerically investigated the pattern formation of granular mixtures on a horizontally oscillating tray and found that a stripe pattern parallel to the oscillating direction is formed for small area fractions of particles. A focus on the formation process of the parallel-striped pattern showed that the particles temporarily form a stripe pattern perpendicular to the oscillating direction of the tray in the early stage; then the perpendicular stripes of large and heavy particles are broken by repeated collisions with actively moving small and light particles, finally resulting in the formation and stabilization of the parallel-striped pattern.

It is notable that Alam and Khalili [15] reported the emergence of parallel-striped patterns in a horizontally oscillating particulate suspension. In the present study, we did not consider the fluid motion; however, these two systems potentially belong to the same universality class in terms of instability of striped pattern formation parallel to a horizontally oscillating external force. The common background mechanism for the emergence of this type of pattern should be explored as the next issue. Also, a more systematic study of the dependency of the final segregation pattern on the elastic constants of the L and S particles remains to be made.

This work is supported by a Research Fellowship of the Japan Society for the Promotion of Science for Young Scientists to M.F., by Grant-in-And for Scientific Research (C) No. 22540391 to H.N., and by the Global COE Program G14 (Formation and Development of Mathematical Sciences Based on Modeling and Analysis) of the Ministry of Education, Culture, Sports, Science and Technology of Japan to H.N..

[1] P. M. Reis, R. A. Ingale, and M. D. Shattuck, Phys. Rev. Lett. **96**, 258001 (2006).
[2] P. M. Reis, G. Ehrhardt, A. Stephenson, and T. Mullin, Europhys. Lett. **66**, 357 (2004).
[3] M. P. Ciamarra, A. Coniglio, and M. Nicodemi, Eur. Phys. J. E **22**, 227 (2007).
[4] G. C. M. A. Ehrhardt, A. Stephenson, and P. M. Reis, Phys. Rev. E **71**, 041301 (2005).
[5] P. M. Reis, T. Sykes, and T. Mullin, Phys. Rev. E **74**, 051306 (2006).
[6] J. Stavans, J. Stat. Phys. **93**, 467 (1998).
[7] O. Zik, D. Levine, S. G. Lipson, S. Shtrikman, and J. Stavans, Phys. Rev. Lett. **73**, 644 (1994).
[8] K. Choo, T. C. A. Molteno, and S. W. Morris, Phys. Rev. Lett. **79**, 2975 (1997).
[9] K. M. Hill, A. Caprihan, and J. Kakalios, Phys. Rev. Lett. **78**, 50 (1997).
[10] A. Awazu, Phys. Rev. Lett. **84**, 4585 (2000).
[11] F. Krzyżewski and M. A. Załuska-Kotur, Phys. Rev. E **77**, 031502 (2008).
[12] P. M. Reis, R. A. Ingale, and M. D. Shattuck, Phys. Rev. E **75**, 051311 (2007).
[13] A. Lipowski and M. Droz, Phys. Rev. E **65**, 031307 (2002).
[14] A. Wysocki and H. Löwen, Phys. Rev. E **79**, 041408 (2009).
[15] M. Alam and A. Khalili, Phys. Rev. E **77**, 041305 (2008).